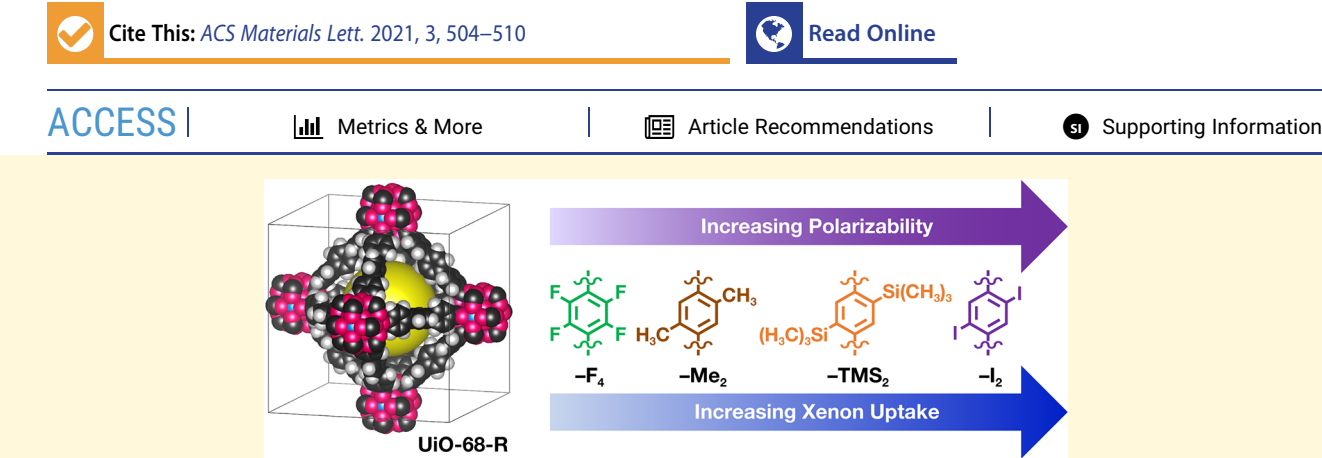


www.acsmaterialsletters.org

Steric and Electronic Effects on the Interaction of Xe and Kr with Functionalized Zirconia Metal—Organic Frameworks

David C. Fairchild, Mohammad I. Hossain, Jesus Cordova, T. Grant Glover,* and Fernando J. Uribe-Romo*



ABSTRACT: The separation of xenon and krypton from their mixtures has been an enduring and complex venture due to their similar sizes and unreactive nature. Metal—organic frameworks (MOFs) have shown the potential to complete these challenging separations by utilizing pressure-swing adsorption (PSA) as a sustainable alternative to current cryogenic distillation techniques. To rationally design materials to better realize this goal, two main approaches have emerged: pore-size optimized and polarizability-based separations. To ascertain the efficacy of these strategies, we designed a series of UiO-type MOFs with terphenyl linkers that systematically varied their steric and electronic properties, including -Me, -F, -TMS, and -I functionalities, to assess their interactions with xenon and krypton. The prepared MOFs are all isoreticular and have similar pore size distributions, allowing us to directly evaluate the effects imposed by the functional groups. We found that the xenon uptake could be increased with greater polarizability of the functional group $(-F < -Me \approx -TMS < -I)$, whereas the selectivities seem to follow a trend more related to pore-steric effects (-TMS < -I < -Me < -F).

¶ he isolation of noble gases from their mixtures is an important challenge in the fields of separations and materials science because of their spherical, monatomic, and highly unreactive natures. ¹⁻³ In particular, the separation of xenon and krypton mixtures, often obtained as off-gases from the reprocessing of spent nuclear fuel (SNF), is of significance due to their different radioactivity, toxicity, and applications as well as the challenges associated with their effective and efficient separation. 4,5 These SNF off-gases contain mixtures of isotopes of krypton and xenon⁶ with varied radioactivity, and special attention must be placed on 85Kr and 133Xe, the most abundant radioisotopes. ^{7,8} 85Kr is a toxic β -emitter, with a long half-life of $t_{1/2}$ = 10.76 years, which should be captured and kept in nuclear waste storage. 8 133 Xe is a much less radioactive eta-emitter, with a much shorter half-life of only $t_{1/2} = 5.243$ days, and is largely depleted by the time of reprocessing.⁸ The recovered xenon has many practical uses in areas such as radiomedicine, lighting, electronics, and ion propulsion.9 Currently, cryogenic distillation is the best-performing and most industrially viable method for the separation of these two gases, but it is an energy expensive process. $^{3,10-12}$

Utilizing pressure-swing adsorption (PSA) is a sustainable alternative to cryogenic distillation, ^{8,13} and porous metal—organic frameworks (MOFs) offer the possibility of addressing this challenge in a systematic manner. ^{3–5,9,12,14–20} Many studies have focused on optimizing different factors of MOFs to achieve efficient separation, such as pore size optimization, ^{5,19,21–24} use of open metal coordination sites, ^{20,24–27} and targeted host—

Received: February 2, 2021 Accepted: March 25, 2021



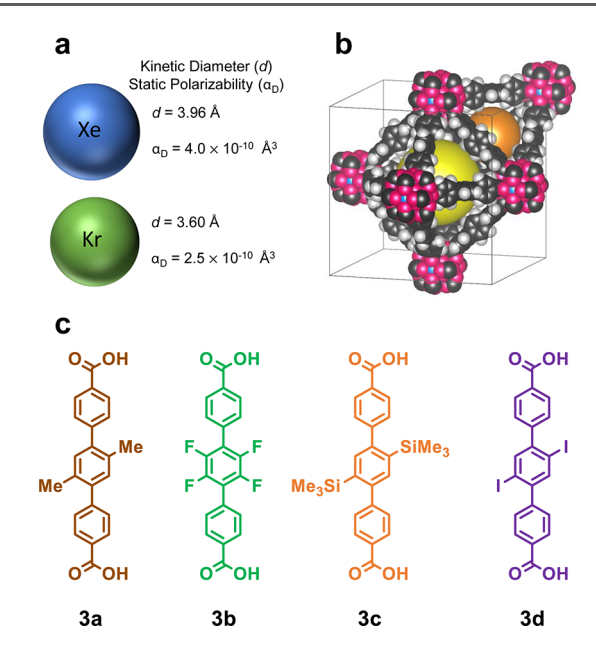


Figure 1. (a) Kinetic diameter and static polarizabilities of xenon and krypton. (b) UiO-68 unit cell showing octahedral and tetrahedral pore (yellow and orange sphere, respectively). (c) Functionalized organic links used in this study.

guest interactions.²⁸ Several materials emphasize precise pore matching to design pores that are slightly larger than the kinetic diameter of xenon (3.96 Å, Figure 1a) to separate these gases.^{3,4,20} For example, MOF-74,²⁹ [Co₃(HCOO)₆]₃₂,¹⁰ SBMOF-1,¹² and CROFOUR-1-Ni³⁰ follow this approach and are some of the best-performing adsorbents so far. More

recently, a squarate-based cobalt MOF, $\mathrm{Co_3C_8H_2O_{10}}^{31}$ attained the highest reported Xe/Kr separation selectivity of 51.4 (based on Henry's law constants from breakthrough experiments in the absence of other competing gases), mainly as a result of the confinement effect from having a pore size of 4.1 Å \times 4.3 Å. This pore-size matching strategy, however, has limitations because of the similar size of both gases, having only a 0.36 Å difference in kinetic diameter (Figure 1a), requiring highly tailored MOF architectures with very precise pore sizes.

An alternative approach is to take advantage of the differences in the electronic properties of the gases, such as exploiting their difference in polarizability (Figure 1a), to favor interaction of one gas with the MOF more than with the other. This idea takes advantage of the "heavy atom effect," where highly polarizable groups interact preferentially with larger atoms (resembling soft-soft interactions). 32-34 The only two systematic studies that address these electronic interactions were performed on monohalogenated derivatives of IRMOF-1 (Zn-based)^{34,35} and functionalized derivatives of UiO-66 (Zr-based).36 The IRMOF-1 study showed that, by including highly polarizable iodine as part of the terephthalate link, higher selectivities were achieved than when functionalizing with Br, Cl, or F, and the UiO-66 study showed a positive correlation between Xe/Kr selectivity and polarized ligands. While these examples have shown high Xe uptake, they result in lower gas selectivity compared to the previous sterics-based methods.

From the viewpoint of physical organic chemistry, where a high degree of synthetic control can be exerted over organic structures, tuning the links of MOFs allows for the possibility of introducing many functional groups to ascertain the nature of their gas separation ability, whether it be steric- or electronic-based. This inspired us to devise a MOF system that is easy to

Scheme 1. Synthesis of Functionalized Organic Links and MOFs

functionalize systematically, stable to humidity, and amenable to sterically demanding groups to understand their type of interactions with Xe and Kr. Here, we prepared a family of UiO-68 derivative MOFs (Figure 1b), composed of water-stable zirconia clusters and terphenyl dicarboxylic acid linkers, that contain pores that range between 10 and 15 Å. To probe differences in both steric and electronic effects, we designed organic links that contain functional groups of varied steric and electronic natures in the central ring of the terphenyl (Figure 1c), specifically: methyl (-Me), fluorine (-F), trimethysilyl (-SiMe₃, -TMS), and iodine (-I) groups. By varying the functional groups on the organic links, we created a series of MOFs (UiO-68-Me₂, UiO-68-F₄, UiO-68-TMS₂, UiO-68-I₂) with the objective of studying their interactions with xenon and krypton to better understand the role of sterics and electronics in these challenging separations. The prepared MOFs are all isoreticular with similar pore size distributions, only differing in the nature of the side groups attached to the linkers. We observed that increased polarizability of the functional group greatly increased the uptake of Xe (UiO-68-F₄ < UiO-68-Me₂ \approx UiO-68-TMS₂ < UiO-68-I₂) while sterics showed a greater effect on the selectivities by increasing the pore size of the MOFs $(UiO-68-TMS_2 < UiO-68-I_2 < UiO-68-Me_2 < UiO-68-F_4)$.

We prepared MOFs isoreticular to UiO-68 whose organic links contain groups of different size and polarizability in the central ring of the terphenyl. These linkers contain -Me (3a), -F(3b), -TMS(3c), and -I(3d) groups, as depicted in Figure 1c. As shown in Scheme 1, $-\text{Me}_2$, $-\text{F}_4$, and $-\text{TMS}_2$ linkers $3\mathbf{a} - \mathbf{c}$ were prepared via Pd-catalyzed Suzuki coupling of dibromobenzene derivatives 1a, 1b, and 1c, respectively, with 4formylphenyl boronic acid (4-FPBA) followed by KMnO₄ oxidation. -I2 linker 3d was prepared via ICl exchange of the TMS group in 2c followed by KMnO₄ oxidation. Oxidation of the aldehydes was chosen as the final step because we found that other intermediates toward carboxylic acids, such as alkyl esters, nitriles, acetyls, or methyls, instead of aldehydes, were prohibitively insoluble, whereas the aldehyde approach provided all the desired linkers with high purities and high yields. Solvothermal crystallization of these linkers in N,N-dimethylformamide (DMF) in the presence of ZrCl₄ and monocarboxylic acid modulators for 2-4 days (Scheme 1; see more in the Supporting Information (SI)) resulted in crystalline materials that exhibit sharp diffraction lines with patterns similar to UiO-68 (Figure 2), confirming the formation of isoreticular frameworks UiO-68-Me2, UiO-68-F4, UiO-68-TMS2, and UiO-68-I₂.

Crystal models of the four MOFs were created using Materials Studio modeling suite³⁷ starting from the crystal structure of UiO-68, adding the specific functional groups for UiO-68-Me₂, UiO-68-TMS₂, and UiO-68-I₂ (ideal symmetry $Fm\overline{3}$) and UiO- $68-F_4$ (ideal symmetry $Fm\overline{3}m$), and then geometry-optimized with the Forcite module using the Universal Force Field (UFF).³⁸ These models were used to perform Rietveld refinement³⁹ of the experimental PXRD patterns, resulting in lattice parameters a = 33.946(16) Å, a = 32.872(4) Å, a =33.261(931) Å, and a = 33.407(13) Å for UiO-68-Me₂, UiO-68-F₄, UiO-68-TMS₂, and UiO-68-I₂, respectively, with low residuals (see the SI). All the MOFs are microporous, as evidenced by their Type II isotherm (Figure 3a), with Brunauer-Emmett-Teller (BET) surface areas of 2600, 2580, 1420 , and $1280 \text{ m}^2 \text{ g}^{-1}$, respectively. We determined the pore size distribution (Figure 3b) using nonlocal density functional theory (NLDFT) methods modeled with the experimental

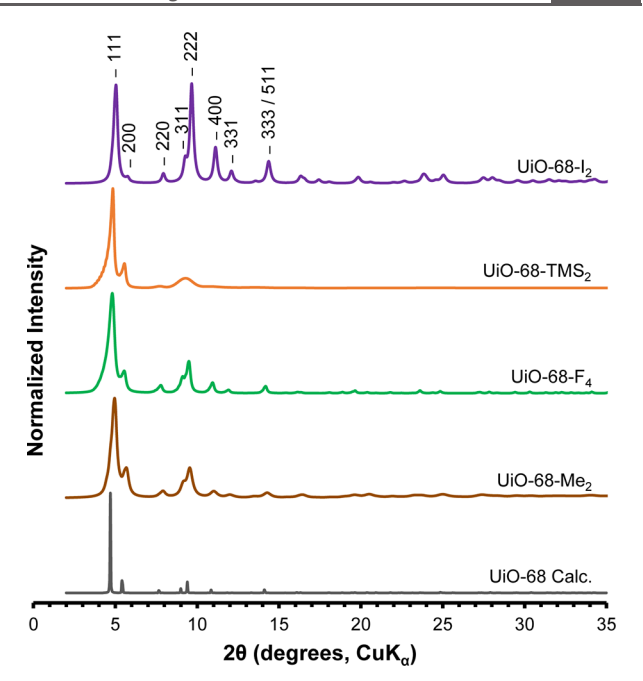
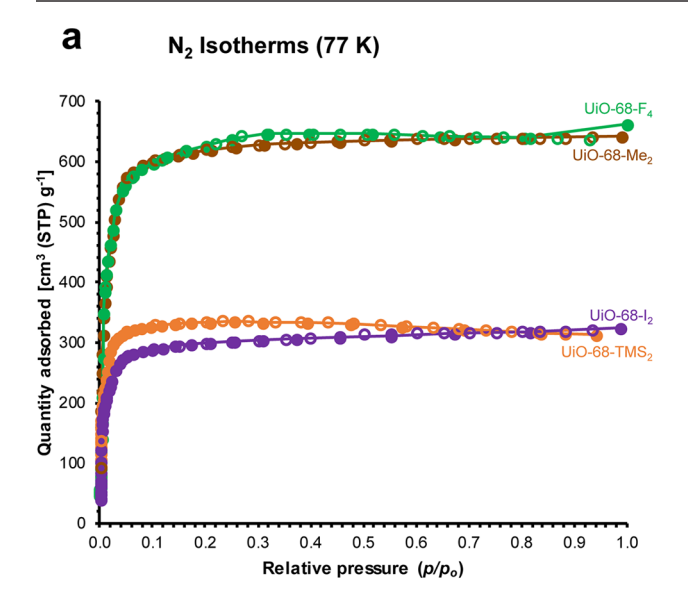


Figure 2. Refined powder X-ray diffractions (PXRDs) of the prepared MOFs, evidencing their isoreticular nature.

isotherms to understand the steric effects that these MOFs cause. All of the MOFs exhibited a bimodal distribution characteristic of the UiO-type MOFs, which contain tetrahedral and octahedral pores (Figure 1b). Interestingly, we observed a very similar pore size distribution in all four MOFs, regardless of the bulkiness of the functional group, likely associated with the small changes in lattice parameter observed, although it is important to note that the NLDFT kernel is only able to approximate the MOF surface, given that it is a metal oxideorganic pore, not a cylindrical oxide pore. This similarity in pore size allowed us to directly observe the trends imposed by the polarizability effects of the functional groups in the adsorption.

When the xenon and krypton isotherms were initially analyzed, the adsorption was quantitatively compared as moles of gas per kilogram of MOF (Figures S19 and S20), as is convention, but we determined that this places too great of an emphasis on the molecular weights of the functional groups, a factor that is not directly responsible in their adsorption capabilities. To account for this, the gas adsorption was compared as moles of gas per mole of MOF unit cells for all gases measured, which has the same value as number of molecules per unit cell. For nitrogen adsorption, the surface areas decrease as a function of how the substituent decreases in size, from TMS < I < Me < F (Figures S17 and S18; Table S2). This trend shows how bulky groups like TMS occupy large portions of the pore resulting in lower uptakes. With respect to Xe/Kr adsorption, as seen in Figure 4, the uptakes increase with increasing polarizability: UiO-68-F₄ < UiO-68-Me₂ \approx UiO-68-TMS₂ < UiO-68-I₂. Also, the sterics imposed by the functionalities have a much lower effect on the uptake, as UiO-68-TMS₂ and UiO-68-Me₂ are very similar in their uptake despite the pore size difference imposed by the groups.

A different trend emerges, however, when comparing the selectivities of xenon over krypton of the MOFs ($S_{\rm Xe/Kr}$) calculated with eq 1:



b Pore Size Distributions

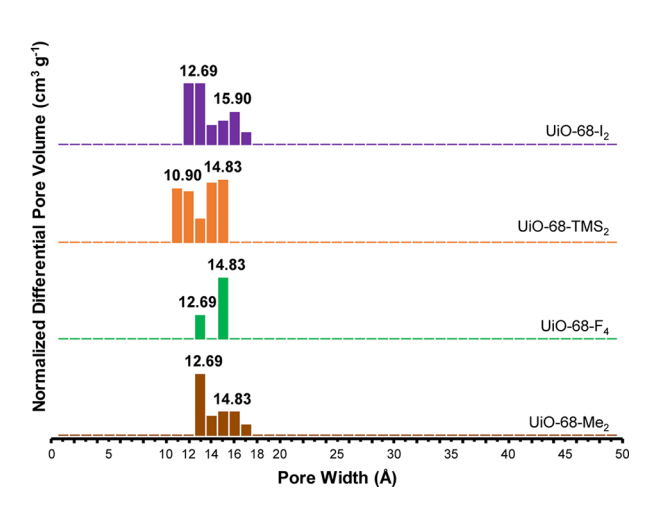
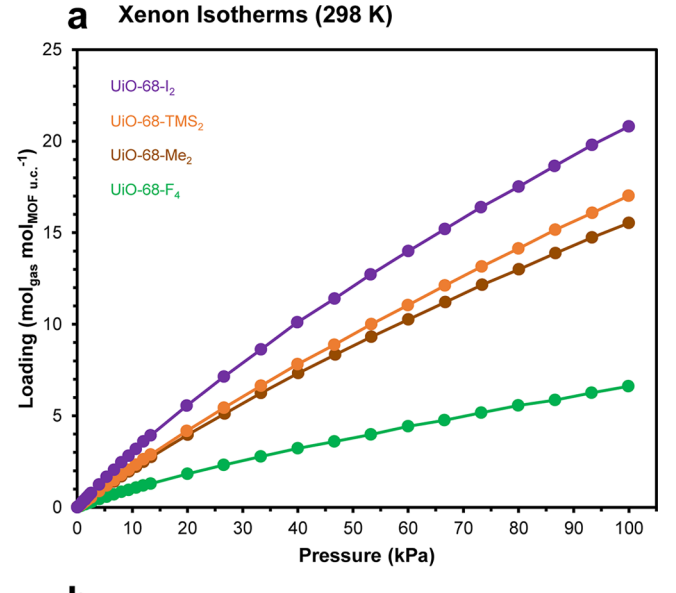


Figure 3. (a) N_2 adsorption isotherms of the prepared MOFs. (b) Pore size distributions determined by NLDFT methods from their respective N_2 isotherms.

$$S_{\text{Xe/Kr}} = \frac{k_{\text{H,Xe}}}{k_{\text{H,Kr}}} \tag{1}$$

where $k_{\rm H}$ corresponds to the Henry's Law constant of adsorption for the respective gas. By calculating the Henry's Law constants at low pressures (0.01–4 kPa), the selectivities follow an increasing trend of UiO-68-TMS $_2$ < UiO-68-I $_2$ < UiO-68-Me $_2$ < UiO-68-F $_4$, with values between 4 and 5 (Table 1). These selectivity values are much lower than those in other MOFs such as CROFOUR-1-Ni 30 or ${\rm Co}_3{\rm C}_8{\rm H}_2{\rm O}_{10}$, 31 which are unfunctionalized and have high selectivity due to their pore sterics. Sikora et al. found from large data simulations of over 137 000 MOFs that the selectivities increase according to a pore-steric effect, improving significantly as the pore size approaches the kinetic diameter of xenon. The pore size range in our MOFs (11–16 Å) is far larger than the optimal theoretical range, 40 so in our materials the Xe/Kr selectivity is dominated only by the pore-steric effects. Previously Meek et al. demonstrated that the IRMOF-2-X series had increased selectivities for the more



Krypton Isotherms (298 K)

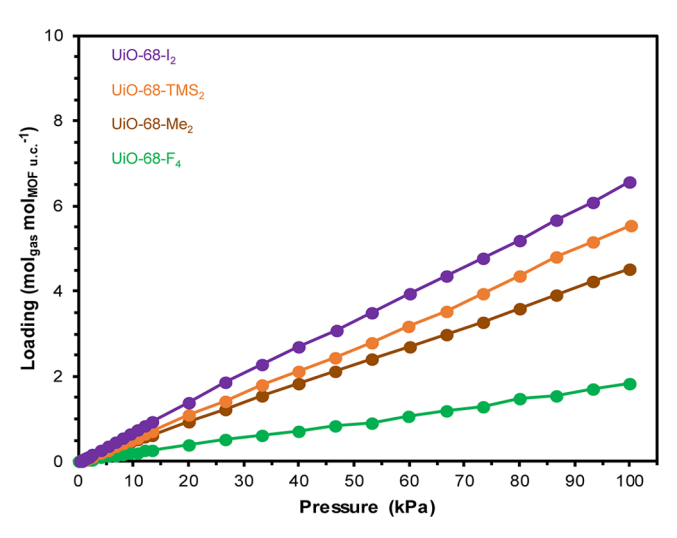


Figure 4. (a) Xe and (b) Kr adsorption isotherms of the functionalized MOFs, measured as a function of moles of gas per mole of MOF.

polarizable monohalogenated linkers.³⁵ For UiO-type MOFs, Lee et al. found that the more donating groups on the linker, the greater the selectivity, while electron-withdrawing groups lower the selectivity.³⁶ The MOFs studied herein do not follow either of these trends, suggesting that the electronic effects are negligible at these pore size ranges, and the variation in the thermodynamic selectivities only ranges from 4.00 (UiO-68-TMS₂) to 4.96 (UiO-68-F₄). A separate study measuring the kinetic selectivities of our MOFs using frequency response or zero-length column experiments may provide additional insight into the design of these types of materials. 41-45 We found that increasing the polarizability of the linkers increases the total Xe uptake without considerable effect from the size of the functional group, whereas the selectivity may be more strongly dependent on the pore-steric effects. The Ideal Adsorbed Solution Theory (IAST) selectivities of all four MOFs at an industrially relevant 20:80 Xe:Kr composition mixture exhibit a similar increasing trend of UiO-68-TMS₂ ($S_{IAST} = 3.86$) < UiO- $68-I_2 (S_{IAST} = 4.25) < UiO-68-Me_2 (S_{IAST} = 4.42) < UiO-68-F_4$ $(S_{IAST} = 5.20)$ as the selectivities calculated from the Henry's law

Table 1. Xe/Kr adsorption uptakes and selectivities

	Uptake at 100 kPa (mol kg ⁻¹)		Henry's law constant, $k_{\rm H}$ (mol kg ⁻¹ kPa ⁻¹)		
MOFs	Xe	Kr	Xe	Kr	Selectivity (from eq 1)
UiO-68-Me ₂	1.41	0.41	1.93×10^{2}	4.23×10^{3}	4.57
UiO-68-F ₄	0.55	0.15	9.39×10^{3}	1.89×10^{3}	4.96
UiO-68-TMS ₂	1.23	0.40	1.60×10^{2}	4.00×10^{3}	4.00
UiO-68-I ₂	1.27	0.40	1.91×10^{2}	4.54×10^{3}	4.21

constant (Figure S27 and Table S3) and are comparable to the IAST selectivities at the same conditions for UiO-66 ($S_{\rm IAST}$ = 6.7), MIL-100 ($S_{\rm IAST}$ = 5.1), and MIL-101 ($S_{\rm IAST}$ = 4.2). ⁴⁶ When attempting to simulate the adsorption isotherms utilizing GCMC calculations, no direct correlation was seen between functional group polarizability, uptake, or selectivity (Figures S25 and S26). These disagreements were similarly observed by Meek et al. and are likely due to the limitations of handling polarizability with the UFF in these types of calculations. ³⁵

In terms of their real-world applications, the MOFs were subjected to water stability and long-term exposure measurements. By comparing the BET surface areas before and after measuring the water vapor isotherms of the MOFs (Figures S28–S31), the stabilities were determined as follows: UiO-68-I₂ < UiO-68-Me₂ < UiO-68-TMS₂ < UiO-68-F₄. The increasing stability of the MOFs is likely related to the hydrophobicity of their functional groups, ⁴⁷ with UiO-68-I₂ having the greatest decrease in its surface area perhaps due to the iodine group having an increased hydrophilicity compared to the other functional groups tested. ⁴⁸ The MOFs were also exposed to the ambient environment for more than 1 month to assess their shelf life stability. Through the comparison of their PXRDs pre- and post-exposure (Figures S32–S35), all the MOFs were shown to maintain their crystallinity, aside from UiO-68-I₂.

In conclusion, a family of functionalized zirconia MOFs was designed to systematically evaluate the effects of steric and electronic properties on their xenon and krypton adsorption and separation capabilities. A positive correlation between the polarizability of the functional group and total xenon uptake was found along with a selectivity trend related to their pore sterics. These results offer a means of identifying MOF characteristics that can be emulated to rationally design linkers for specific applications in these challenging separations and provide a basis for the development of MOFs for use in PSA as a sustainable alternative for noble gas separations.

ASSOCIATED CONTENT

Supporting Information

The Supporting Information is available free of charge at https://pubs.acs.org/doi/10.1021/acsmaterialslett.1c00077.

Crystallographic information for UiO-68-Me₂ (CIF) Crystallographic information for UiO-68-F₄ (CIF) Crystallographic information for UiO-68-TMS₂ (CIF) Crystallographic information for UiO-68-I₂ (CIF) Materials and methods, synthesis procedures, X-ray diffraction, SEM images, gas adsorption measurements, stability studies, thermogravimetric and spectroscopic analysis, and NMR spectra (PDF)

AUTHOR INFORMATION

Corresponding Authors

Fernando J. Uribe-Romo — Department of Chemistry and Renewable Energy and Chemical Transformations Cluster, University of Central Florida, Orlando, Florida 32816-2366, United States; orcid.org/0000-0003-0212-0295; Email: fernando@ucf.edu

T. Grant Glover — Department of Chemical and Biomolecular Engineering, University of South Alabama, Mobile, Alabama 36677, United States; Occid.org/0000-0002-3393-6038; Email: glover@southalabama.edu

Authors

David C. Fairchild – Department of Chemistry and Renewable Energy and Chemical Transformations Cluster, University of Central Florida, Orlando, Florida 32816-2366, United States; © orcid.org/0000-0003-4069-6471

Mohammad I. Hossain — Department of Chemical and Biomolecular Engineering, University of South Alabama, Mobile, Alabama 36677, United States; ⊚ orcid.org/0000-0003-0315-709X

Jesus Cordova – Department of Chemistry, University of Central Florida, Orlando, Florida 32816-2366, United States

Complete contact information is available at: https://pubs.acs.org/10.1021/acsmaterialslett.1c00077

Author Contributions

The manuscript was written through contributions of all authors. All authors have given approval to the final version of the manuscript.

Funding

X-ray characterization of materials was partially funded by the National Science Foundation (CHE-1665277, FJU-R).

Notes

The authors declare no competing financial interest.

ACKNOWLEDGMENTS

We would like to thank Dr. Laurene Tetard (UCF) for technical assistance.

■ REFERENCES

- (1) Chen, L.; Reiss, P. S.; Chong, S. Y.; Holden, D.; Jelfs, K. E.; Hasell, T.; Little, M. A.; Kewley, A.; Briggs, M. E.; Stephenson, A.; Thomas, K. M.; Armstrong, J. A.; Bell, J.; Busto, J.; Noel, R.; Liu, J.; Strachan, D. M.; Thallapally, P. K.; Cooper, A. I. Separation of Rare Gases and Chiral Molecules by Selective Binding in Porous Organic Cages. *Nat. Mater.* **2014**, *13*, 954–960.
- (2) Greathouse, J. A.; Kinnibrugh, T. L.; Allendorf, M. D. Adsorption and Separation of Noble Gases by IRMOF-1: Grand Canonical Monte Carlo Simulations. *Ind. Eng. Chem. Res.* **2009**, *48*, 3425–3431.
- (3) Banerjee, D.; Cairns, A. J.; Liu, J.; Motkuri, R. K.; Nune, S. K.; Fernandez, C. A.; Krishna, R.; Strachan, D. M.; Thallapally, P. K. Potential of Metal-Organic Frameworks for Separation of Xenon and Krypton. *Acc. Chem. Res.* **2015**, *48*, 211–219.
- (4) Liu, J.; Fernandez, C. A.; Martin, P. F.; Thallapally, P. K.; Strachan, D. M. A Two-Column Method for the Separation of Kr and Xe from Process Off-Gases. *Ind. Eng. Chem. Res.* **2014**, *53*, 12893–12899.
- (5) Anderson, R.; Schweitzer, B.; Wu, T.; Carreon, M. A.; Gómez-Gualdrón, D. A. Molecular Simulation Insights on Xe/Kr Separation in

- a Set of Nanoporous Crystalline Membranes. ACS Appl. Mater. Interfaces 2018, 10, 582-592.
- (6) Kerry, F. G. Industrial Gas Handbook: Gas Separation and Purification; CRC Press, 2007.
- (7) Fontaine, J.-P.; Pointurier, F.; Blanchard, X.; Taffary, T. Atmospheric Xenon Radioactive Isotope Monitoring. *J. Environ. Radioact.* **2004**, *72*, 129–135.
- (8) Chen, J.; Hsu, S.-J.; Wei, T.-Y. Optimization Design for Removal of radioactive Kr from Xe using Pressure Swing Adsorption. *Chem. Eng. Res. Des.* **2013**, *91*, 649–659.
- (9) Banerjee, D.; Simon, C. M.; Elsaidi, S. K.; Haranczyk, M.; Thallapally, P. K. Xenon Gas Separation and Storage Using Metal-Organic Frameworks. *Chem.* **2018**, *4*, 466–494.
- (10) Wang, H.; Yao, K.; Zhang, Z.; Jagiello, J.; Gong, Q.; Han, Y.; Li, J. The First Example of Commensurate Adsorption of Atomic Gas in a MOF and Effective Separation of Xenon from Other Noble Gases. *Chem. Sci.* **2014**, *5*, 620–624.
- (11) Chen, X.; Plonka, A. M.; Banerjee, D.; Krishna, R.; Schaef, H. T.; Ghose, S.; Thallapally, P. K.; Parise, J. B. Direct Observation of Xe and Kr Adsorption in a Xe-Selective Microporous Metal-Organic Framework. J. Am. Chem. Soc. 2015, 137, 7007—7010.
- (12) Banerjee, D.; Simon, C. M.; Plonka, A. M.; Motkuri, R. K.; Liu, J.; Chen, X.; Smit, B.; Parise, J. B.; Haranczyk, M.; Thallapally, P. K. Metal-Organic Framework with Optimally Selective Xenon Adsorption and Separation. *Nat. Commun.* **2016**, *7*, ncomms11831.
- (13) Mueller, U.; Schubert, M.; Teich, F.; Puetter, H.; Schierle-Arndt, K.; Pastré, J. Metal-Organic Frameworks—Prospective Industrial Applications. J. Mater. Chem. 2006, 16, 626–636.
- (14) Zhao, D.; Timmons, D. J.; Yuan, D.; Zhou, H.-C. Tuning the Topology and Functionality of Metal-Organic Frameworks by Ligand Design. *Acc. Chem. Res.* **2011**, *44*, 123–133.
- (15) Lu, W.; Wei, Z.; Gu, Z.-Y.; Liu, T.-F.; Park, J.; Park, J.; Tian, J.; Zhang, M.; Zhang, Q.; Gentle, T., III; Bosch, M.; Zhou, H.-C. Tuning the Structure and Function of Metal-Organic Frameworks via Linker Design. *Chem. Soc. Rev.* **2014**, *43*, 5561–5593.
- (16) Yuan, S.; Chen, Y.-P.; Qin, J.-S.; Lu, W.; Zou, L.; Zhang, Q.; Wang, X.; Sun, X.; Zhou, H.-C. Linker Installation: Engineering Pore Environment with Precisely Placed Functionalities in Zirconium MOFs. J. Am. Chem. Soc. 2016, 138, 8912–8919.
- (17) Vazhappilly, T.; Ghanty, T. K.; Jagatap, B. N. Computational Modeling of Adsorption of Xe and Kr in M-MOF-74 Metal-Organic Frameworks with Different Metal Atoms. *J. Phys. Chem. C* **2016**, *120*, 10968–10974.
- (18) Mellot-Draznieks, C. Computational Exploration of Metal-Organic Frameworks: Examples of Advances in Crystal Structure Predictions and Electronic Structure Tuning. *Mol. Simul.* **2015**, *41*, 1422–1437.
- (19) Parkes, M. V.; Staiger, C. L.; Perry, J. J., IV; Allendorf, M. D.; Greathouse, J. A. Screening Metal-Organic Frameworks for Selective Noble Gas Adsorption in Air: Effect of Pore Size and Framework Topology. *Phys. Chem. Chem. Phys.* **2013**, *15*, 9093–9106.
- (20) Perry, J. J.; Teich-McGoldrick, S. L.; Meek, S. T.; Greathouse, J. A.; Haranczyk, M.; Allendorf, M. D. Noble Gas Adsorption in Metal-Organic Frameworks Containing Open Metal Sites. *J. Phys. Chem. C* **2014**, *118*, 11685–11698.
- (21) Li, J.-R.; Kuppler, R. J.; Zhou, H.-C. Selective Gas Adsorption and Separation in Metal-Organic Frameworks. *Chem. Soc. Rev.* **2009**, 38, 1477–1504.
- (22) Czaja, A. U.; Trukhan, N.; Müller, U. Industrial Applications of Metal-Organic Frameworks. *Chem. Soc. Rev.* **2009**, *38*, 1284–1293.
- (23) Idrees, K. B.; Chen, Z.; Zhang, X.; Rasel Mian, M.; Drout, R. J.; Islamoglu, T.; Farha, O. K. Tailoring Pore Aperture and Structural Defects in Zirconium-based Metal-Organic Frameworks for Krypton/Xenon Separation. *Chem. Mater.* **2020**, *32*, 3776–3782.
- (24) Xue, D.-X.; Belmabkhout, Y.; Shekhah, O.; Jiang, H.; Adil, K.; Cairns, A. J.; Eddaoudi, M. Tunable Rare Earth fcu-MOF Platform: Access to Adsorption Kinetics Driven Gas/Vapor Separations via Pore Size Contraction. *J. Am. Chem. Soc.* **2015**, *137*, 5034—5040.

- (25) Thallapally, P. K.; Grate, J. W.; Motkuri, R. K. Facile Xenon Capture and Release at Room Temperature Using a Metal-Organic Framework: A Comparison with Activated Charcoal. *Chem. Commun.* **2012**, *48*, 347–349.
- (26) Wu, X.-L.; Li, Z.-J.; Zhou, H.; Yang, G.; Liu, X.-Y.; Qian, N.; Wang, W.; Zeng, Y.-S.; Qian, Z.-H.; Chu, X.-X.; Liu, W. Enhanced Adsorption and Separation of Xenon over Krypton via an Unsaturated Calcium Center in a Metal-Organic Framework. *Inorg. Chem.* **2021**, *60*, 1506–1512.
- (27) Wang, H.; Shi, Z.; Yang, J.; Sun, T.; Rungtaweevoranit, B.; Lyu, H.; Zhang, Y.-B.; Yaghi, O. M. Docking of Cu(I) and Ag(I) in Metal-Organic Frameworks for Adsorption and Separation of Xenon. *Angew. Chem., Int. Ed.* **2021**, *60*, 3417–3421.
- (28) Liu, J.; Strachan, D. M.; Thallapally, P. K. Enhanced Noble Gas Adsorption in Ag@MOF-74Ni. Chem. Commun. 2014, 50, 466–468.
- (29) Liu, J.; Thallapally, P. K.; Strachan, D. Metal-Organic Frameworks for removal of Xe and Kr from Nuclear Fuel Reprocessing Plants. *Langmuir* **2012**, 28, 11584–11589.
- (30) Mohamed, M. H.; Elsaidi, S. K.; Pham, T.; Forrest, K. A.; Schaef, H. T.; Hogan, A.; Wojtas, L.; Xu, W.; Space, B.; Zaworotko, M. J.; Thallapally, P. K. Hybrid Ultra-Microporous Materials for Selective Xenon Adsorption and Separation. *Angew. Chem., Int. Ed.* **2016**, *55*, 8285–8289.
- (31) Li, L.; Guo, L.; Zhang, Z.; Yang, Q.; Yang, Y.; Bao, Z.; Ren, Q.; Li, J. A Robust Squarate-Based Metal-Organic Framework Demonstrates Rcord-High Affinity and Selectivity for Xenon over Krypton. *J. Am. Chem. Soc.* **2019**, *141*, 9358–9364.
- (32) Bloch, E. D.; Queen, W. L.; Krishna, R.; Zadrozny, J. M.; Brown, C. M.; Long, J. R. Hydrocarbon Separations in a Metal-Organic Framework with Open Iron(II) Coordination Sites. *Science* **2012**, 335, 1606–1610.
- (33) Mulfort, K. L.; Hupp, J. T. Chemical Reduction of Metal-Organic Framework Materials as a Method to Enhance Gas Uptake and Binding. *J. Am. Chem. Soc.* **2007**, *129*, 9604–9605.
- (34) Meek, S. T.; Perry, J. J., IV; Teich-McGoldrick, S. L.; Greathouse, J. A.; Allendorf, M. D. Complete Series of Monohalogenated Isoreticular Metal-Organic Frameworks: Synthesis and the Importance of Activation Method. *Cryst. Growth Des.* **2011**, *11*, 4309–4312.
- (35) Meek, S. T.; Teich-McGoldrick, S. L.; Perry, J. J., IV; Greathouse, J. A.; Allendorf, M. D. Effects of Polarizability on the Adsorption of Noble Gases at Low Pressures in Monohalogenated Isoreticular Metal-Organic Frameworks. *J. Phys. Chem. C* **2012**, *116*, 19765–19772.
- (36) Lee, S.-J.; Kim, S.; Kim, E.-J.; Kim, M.; Bae, Y.-S. Adsorptive Separation of Xenon/Krypton Mixtures Using Ligand Controls in a Zirconium-Based Metal-Organic Framework. *Chem. Eng. J.* **2018**, 335, 345–351.
- (37) Dassault Systèmes BIOVIA. *Materials Studio*, 5.5.2; Dassault Systèmes: San Diego, 2020.
- (38) Rappe, A. K.; Casewit, C. J.; Colwell, K. S.; Goddard, W. A.; Skiff, W. M. UFF, a Full Periodic Table Force Field for Molecular Mechanics and Dynamics Simulations. *J. Am. Chem. Soc.* **1992**, *114*, 10024–10035.
- (39) Toby, B. H.; Von Dreele, R. B. GSAS-II: The Genesis of a Modern Open-Source All Purpose Crystallography Software Package. *J. Appl. Crystallogr.* **2013**, *46*, 544–549.
- (40) Sikora, B. J.; Wilmer, C. E.; Greenfield, M. L.; Snurr, R. Q. Thermodynamic Analysis of Xe/Kr Selectivity in Over 137,000 Hypothetical Metal-Organic Frameworks. *Chem. Sci.* **2012**, *3*, 2217–2223.
- (41) Glover, T. G.; Mu, B. Gas Adsorption in Metal-Organic Frameworks: Fundamentals and Applications; CRC Press, 2018.
- (42) Hossain, M. I.; Glover, T. G. Kinetics of Water Adsorption in UiO-66 MOF. *Ind. Eng. Chem. Res.* **2019**, *58*, 10550–10558.
- (43) Tovar, T. M.; Zhao, Z.; Nunn, W. T.; Barton, H. F.; Peterson, G. W.; Parsons, G. N.; LeVan, M. D. Diffusion of CO₂ in Large Crystals of Cu-BTC MOF. *J. Am. Chem. Soc.* **2016**, 138, 11449–11452.
- (44) Wang, Y.; Paur, C. S.; Ravikovitch, P. I. New Development in Flow-Through Pressure-Swing Frequency Response Method for Mass-Transfer Study: Ethane in ZIF-8. *AIChE J.* **2017**, *63*, 1077–1090.

- (45) Hu, X.; Brandani, S.; Benin, A. I.; Willis, R. R. Development of a Semiautomated Zero Length Column Technique for Carbon Capture Applications: Study of Diffusion Behavior of CO₂ in MOFs. *Ind. Eng. Chem. Res.* **2015**, *54*, 5777–5783.
- (46) Lee, S.-J.; Yoon, T.-U.; Kim, A.-R.; Kim, S.-Y.; Cho, K.-H.; Hwang, Y. K.; Yeon, J.-W.; Bae, Y.-S. Adsorptive Separation of Xenon/Krypton mixtures Using a Zirconium-based Metal-Organic Framework with High Hydrothermal and Radioactive Stabilities. *J. Hazard. Mater.* **2016**, *320*, 513–520.
- (47) Sata, T.; Mine, K.; Tagami, Y.; Higa, M.; Matsusaki, K. Changing Permselectivity Between Halogen Ions Through Anion Exchange Membranes in Electrodialysis by Controlling Hydrophilicity of the Membranes. *J. Chem. Soc., Faraday Trans.* **1998**, *94*, 147–153.
- (48) Logan, M. W.; Adamson, J. D.; Le, D.; Uribe-Romo, F. J. Structural Stability of N-Alkyl-Functionalized Titanium Metal-Organic Frameworks in Aqueous and Humid Environments. *ACS Appl. Mater. Interfaces* **2017**, *9*, 44529–44533.